EFFECT OF BEDDING PLANES ON ROCK MECHANICAL PROPERTIES ANISOTROPY OF SANDSTONE FOR GEOMECHANICAL MODELING

Dee Moronkeji, Richard Shouse and Umesh Prasad
Baker Hughes, Houston, TX, USA

This paper was prepared for presentation at the International Symposium of the Society of Core Analysts held in Snowmass, Colorado, USA, 21-26 August 2016

ABSTRACT
Side wall cores have become a routine coring operation in conventional and unconventional formations. The recent departure from drilling vertical wells to directional drilling of wellbores in unconventional wells has led to side wall cores that are acquired in different directions to bedding planes. Studies have shown that rock mechanical properties can be affected by bedding planes. Consequently, side wall cores retrieved from unconventional wells that are used for rock mechanical properties (RMP) estimation for geomechanical modelling can lead to unrealistic models, depending on the coring direction.

The main purpose of this study is to examine the effect of bedding planes on RMP, especially from side wall cores. Depending on the well inclination to the bedding plane, core plugs are taken along three orthogonal directions and at intermediate orientation with respect to bedding and tested at unconfined and confined conditions to obtain unconfined compressive strength (UCS) and confined compressive strength (CCS) for sandstone samples with bedding planes.

This study is an effort to characterize strength anisotropy using orthotropic considerations and to examine the source of anisotropy and determine if it is stress induced. Berea sandstone with bedding planes was selected to perform a series of UCS and CCS tests. The rock strength was observed to be highest in the plugs drilled perpendicular to bedding (ZZ) and consistently lowest in the horizontal plugs drilled parallel across the bedding (YY) compared to the horizontal plugs drilled parallel along (XX) the beddings. The difference in the rock strength measured in the plugs parallel along and across the bedding could be due to the pre-existing stress anisotropy and can be a clue to the horizontal stress orientation in bedded formations as result of depositional environment and existing tectonic stresses.

This knowledge will help in planning coring operations, completion, and production processes and better sand production prediction in bedded formation with significant bedding plane in which side wall cores are taken that can significantly alter the RMP and geomechanical modeling predictions.

INTRODUCTION
Rock mechanical properties are key parameters in geomechanical models and their subsequent use to plan and design drilling, evaluation, completion, and production

processes. RMP such as elastic properties of Young's modulus (EMOD) and Poisson's ratio (PR) and UCS or CCS are regularly used for geomechanical investigation, and assume rocks to be continuous, homogenous, linearly elastic and isotropic. Traditionally, isotropic considerations can be assumed based on the level of variation in RMP of elastic and peak strength beyond an accepted threshold level (say 5% or 10%). However, if the variation is beyond the threshold level, an anisotropic consideration has to be applied, originating from vertical transverse isotropy (VTI) or orthotropic considerations. Luckily, the recent technological advancement of dipole or quadrupole acoustics has enabled the industry to characterize the VTI anisotropic behavior from logs together with laboratory-based measurements to supplement or calibrate log measurements. Orthotropic considerations have also been tried based on extensive lab-based measurements, but their use has been limited because they require extensive lab testing to supplement the log measurements.

Studies have shown that RMP can be affected significantly due to intrinsic features such as laminations, foliations, bedding planes or extrinsic stressed-induced anisotropy. Due care should be taken to utilize the typical rock mechanical behavior in deciding drilling trajectory, quantifying suitable mud weight windows for mitigating wellbore stability issues, or planning and design of perforation or hydraulic fracturing.

The effect of bedding planes as a source of intrinsic properties on strength and elastic properties on sedimentary rocks carried out on vertical, inclined, or horizontal plugs are discussed in detail by Jaeger and Cook [1], and Zoback [2]. Other earlier work on shale, sandstone and limestone was performed by Chenevert, M. and Gatlin, C. [3] and McLamore, R. and Gray, K. [4] on slate. However, very limited work has been done to characterize full anisotropy, especially in visually isotropic looking sandstone. Some study on anisotropy in sandstone was performed by Holt, R.M et al. [5] and Yasar [6].

TESTING PROGRAM

A large number of core plugs were taken according to the direction of bedding plane and loading direction (plug axis). The plugs were drilled from the same Berea sandstone block to examine if the RMP would be different (see Figure 1) and grouped according to the orientation of the loading direction with respect to the bedding plane.

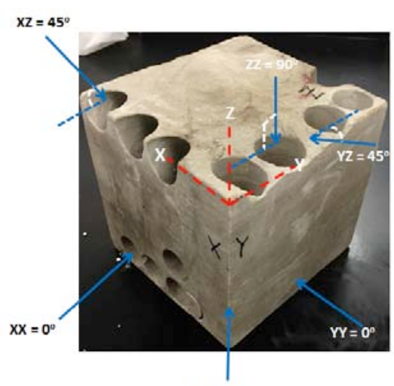

Figure 1: Berea Sandstone Block with Drilling Directions with Respect to Bedding Plane

The ZZ axis (90^o) is perpendicular to horizontal bedding, XX, YY and XY (0^o), are parallel along (X-axis), across (Y-axis) and inclined (45°) on the horizontal plane to the bedding, respectively, XZ and YZ (45^o) are inclined along and across the bedding, respectively.

The bulk density of all plugs was measured. Mineralogical and microstructural properties were measured by X-ray diffraction (XRD) and scanning electron microscope (SEM) on selected samples to see the samples mineralogical composition homogeneity. UCS and CCS tests at 5500 psi confining pressure were carried out using a TerraTek 880 triaxial load frame with an MTS servo-digital control system, confining pressure intensifier, hydraulic service manifold, and a Silent-flow hydraulic power unit. The tests met the ASTM standard D4543-04 [7].

Axial and radial strain measurements were performed using linear variable displacement transducers and a circumferential extensometer, respectively, at a circumferential strain rate of 1.69 x 10^{-5} cm/sec. (0.0004-in./min.) for all tests.

RESULTS

The SEM analysis on the Berea sandstone shows that there are pore-filling vermiculites of kaolinite and corroded sodium feldspar. The vermiculites, confirmed by using XRD, as 4% kaolinite with the Berea sandstone predominantly composed of 88% quartz minerals. The XRD result is shown in Table 1 and the SEM plots are shown in Figure 2.

The results of the triaxial testing at UCS and CSS are shown in Table 1 for all orientations with a standard deviation of one. The perpendicular sample has the highest peak strength in UCS and CCS tests than the parallel or inclined samples, showing that strength anisotropy is also present under confining conditions. This was also observed by Holt, R. M., et al. [5] and Zetian Zhang et al. [8] as it is more difficult for the failure plane to develop and cross through (perpendicular) the bedding plane than it is to develop along (parallel) the bedding plane as shown by the axial strain at failure in Table 1. The standard deviation shows that statistically the errors were 8% and 4% on the vertical and horizontal plugs with an average UCS of 48 MPa and 38 MPa in ZZ and XX, respectively, except in the YY (15% difference), where the error was even lower in CCS with 2% and 1%, respectively, for the ZZ and XX direction, showing good testing repeatability.

Figure 3 for the UCS and CCS tests, respectively, show that the YY samples peak strength, with average values of 33 and 186 MPa, is lower than the 38 and 191 MPa in the XX. This shows that strength anisotropy exists in bedded Berea sandstone.

It can be assumed to be either a VTI or orthotropic rock. If we ignore the outlier from the XX and YY data sets and take only two concurrent values, then it further shows that YY cores are weakest. UCS, CCS and EMOD at 0 psi and 5500 psi show that this can only be explained that there is one plane of symmetry, so the pre-existing stress condition must be the cause of the weaker plane along YY. The weakest YY is also evident from CCS and EMOD data. Figure 4 show that EMOD increases linearly with the UCS at each plug orientation to bedding, and as a whole with a high linear regression correlation (R^2 of 0.85). A similar observation is also seen for the CCS. The effect of bedding planes on EMOD shown in Figure 5 for UCS and CCS were higher in the perpendicular direction to

bedding (90^o) compared to the other directions. This was also observed by Zetian Zhang et al. [8] in their testing.
Figure 6 shows there are no distinct patterns of the shear plane failure based on the loading direction with respect to the bedding orientation; all samples show a clear shear failure plane. A typical stress-strain plot is shown in Figure 7 at three directions (ZZ, XX and YY) with respect to bedding. The plot clearly shows that the CCS is clearly lower on the YY than in the other directions.

CONCLUSION

The testing results show that it is possible that the stress anisotropy and bedding direction of oriented cores can indicate the direction of the principal stresses due to
pre-existing stress orientations. The maximum stress direction caused ZZ to be the strongest. Further, if we ignore the outlier, YY was the weakest. This could only be explained by the influence of intermediate or least principal stress influence in alignment of foliation or microcracks.
The stress anisotropy inferred by the testing in the Berea sandstone clearly shows that anisotropic consideration should be used in bedded sandstones formation as indicated by the results because bedded sandstone formation are more stress sensitive.
Future testing will include conducting P&S wave measurements, to see if the non-destructive testing can also validate the finding in this testing program, and applying this methodology to a wellbore with known stress orientation. Finally, the data obtained will help in planning coring operations in the bedded formation because the strength anisotropy measured can be a clue to the in-situ stress orientation and help in building realistic geomechanical model in these types of formations.

ACKNOWLEDGEMENTS

The authors would like to thank Baker Hughes for the permission to publish the results. We also thank Amber Koch and BJ Davis for the XRD & SEM testing and interpretation.

REFERENCES

1. T Jaeger, JC & NGW Cook; 1979. Fundamentals of Rock Mechanics. Chapman & Hall.
2. Zoback, M.D.; 2008. Reservoir Geomechanics, Cambridge University Press.
3. Chenevert, M.E. and C. Gatlin. 1964. Mechanical anisotropies of laminated sedimentary rocks. 39th Annual SPE Meeting, Houston, TX., Oct. 11-14. 67–77.
4. McLamore, R.T. and K.E. Gray. 1967. A Strength Criterion for Anisotropic Rocks Based Upon Experimental Observations. 96th Annual AIME Meeting, Los Angeles, California, Feb. 19-23. SPE 1721.
5. Holt, R. M., et al., 1987. Anisotropic Mechanical Properties of Weakly Consolidated Sandstone. ISRM Congress 177.
6. Yasar, E. 2001. Failure and Failure Theories for Anisotropic Rocks. 17th international Mining Congress and Exhibition of Turkey- IMCET 2001.
7. ASTM, 2004. Standard Practices for Preparing Rock Core Specimens & Determining Dimensional and Shape Tolerances. D4543-04. Annual Book of ASTM Standards.

8. Zetian Zhang et al. (2014). Effect of Bedding Structure on Mechanical Property of Coal. *Advances in Materials Science and Engineering, Volume 2014, Article 952703.*

Table 1. Berea Sandstone UCS and CCS Triaxial Test Results and XRD Analysis

Sample ID	Sample Orientation		D	L	Den	UCS	EMOD	PR	Strain corresponding to Peak Stress (in)			STDEV UCS	STDEV EMOD	STDEV POIS
	X-Y-Z	Deg	in	in	g/cc	MPa	GPa		Axial Strain	Circum. strain	Volum. strain	MPa	GPa	
UCS														
BV-5	ZZ	90	1.00	1.99	2.17	44.0	11.2	0.25	0.0049	-0.0019	0.0010	3.8	0.7	0.03
BV-2	ZZ	90	0.99	1.96	2.17	47.5	11.3	0.21	0.0050	-0.0014	0.0022			
BV-3	ZZ	90	0.98	1.95	2.20	51.6	12.4	0.26	0.0059	-0.0021	0.0017			
Average			0.99	1.96	2.18	47.7	11.6	0.24	0.0052	-0.0018	0.0016			
HC-6	XX	0	0.98	1.96	2.21	36.6	10.0	0.28	0.0042	-0.0022	-0.0002	1.5	0.6	0.05
HC-3	XX	0	1.00	1.97	2.19	37.9	11.1	0.30	0.0040	-0.0019	0.0002			
HC-2	XX	0	0.99	1.98	2.18	39.6	10.9	0.37	0.0041	-0.0029	-0.0017			
Average			0.99	1.97	2.20	38.0	10.7	0.32	0.0041	-0.0023	-0.0006			
HB-4	YY	0	0.99	2.01	2.12	27.2	7.6	0.19	0.0047	-0.0028	-0.0008	4.9	1.2	0.05
HB-2	YY	0	0.99	1.90	2.11	34.5	9.4	0.28	0.0047	-0.0024	0.0000			
HB-6	YY	0	1.00	2.03	2.17	36.6	10.0	0.27	0.0045	-0.0024	-0.0004			
Average			0.99	1.98	2.13	32.7	9.0	0.25	0.0046	-0.0025	-0.0004			
ID-1	XY	0	1.00	1.95	2.17	36.7	10.9	0.29	0.0042	-0.0021	0.0000	2.2	1.0	0.07
ID-3	XY	0	0.99	1.94	2.16	33.3	9.1	0.34	0.0036	-0.0016	0.0003			
ID-5	XY	0	0.99	2.01	2.16	32.5	9.1	0.20	0.0045	-0.0014	0.0016			
Average			0.99	1.97	2.16	34.2	9.7	0.28	0.0041	-0.0017	0.0006			
IC-2	XZ	45	1.00	1.95	2.17	34.9	10.0	0.26	0.0042	-0.0020	0.0002	4.8	0.9	0.02
IC-1	XZ	45	1.00	2.04	2.15	42.0	11.5	0.26	0.0046	-0.0021	0.0004			
IC-8	XZ	45	0.99	1.96	2.21	44.0	11.6	0.22	0.0051	-0.0014	0.0023			
Average			1.00	1.99	2.17	40.3	11.0	0.24	0.0046	-0.0018	0.0010			
IB-5	YZ	45	0.99	1.95	2.18	37.1	9.8	0.21	0.0048	-0.0014	0.0020	5.2	1.1	0.03
IB-1	YZ	45	0.98	1.90	2.15	41.6	10.5	0.25	0.0052	-0.0036	-0.0021			
IB-4	YZ	45	0.99	1.99	2.18	47.5	11.9	0.26	0.0054	-0.0021	0.0011			
Average			0.99	1.95	2.17	42.0	10.7	0.24	0.0051	-0.0024	0.0003			
5500 psi Confining														
BV-4	ZZ	90	1.00	1.97	2.19	191.8	17.5	0.11	0.0114	-0.0015	0.0085	3	1.0	0.02
BV-6	ZZ	90	1.00	2.04	2.19	192.6	18.2	0.08	0.0122	-0.0039	0.0043			
BV-8	ZZ	90	0.99	1.99	2.22	197.7	19.6	0.13	0.0092	-0.0015	0.0063			
Average			0.99	2.00	2.20	194.0	18.4	0.11	0.0109	-0.0023	0.0064			
HC-8	XX	0	0.99	1.98	2.16	188.6	16.6	0.14	0.0119	-0.0024	0.0071	3	0.4	0.01
HC-7	XX	0	0.99	1.89	2.18	191.9	16.7	0.13	0.0122	-0.0026	0.0071			
HC-5	XX	0	0.99	1.96	2.24	193.8	17.2	0.15	0.0112	-0.0023	0.0065			
Average			0.99	1.94	2.19	191.4	16.8	0.14	0.0118	-0.0024	0.0069			
HB-5	YY	0	0.99	1.98	2.19	173.2	16.9	0.11	0.0107	-0.0015	0.0076	11	0.8	0.06
HB-1	YY	0	0.98	1.92	2.19	188.9	17.0	0.23	0.0119	-0.0021	0.0078			
HB-8	YY	0	0.99	1.83	2.19	194.4	18.4	0.13	0.0106	-0.0020	0.0067			
Average			0.99	1.91	2.19	185.5	17.4	0.15	0.0110	-0.0018	0.0074			
ID-2	XY	0	0.99	1.88	2.14	173.8	17.0	0.12	0.0110	-0.0021	0.0069	1	0.3	0.01
ID-4	XY	0	0.99	1.95	2.18	175.4	16.5	0.13	0.0116	-0.0022	0.0071			
Average			0.99	1.92	2.16	174.6	16.8	0.13	0.0113	-0.0022	0.0070			
IC-5	XZ	45	1.00	1.96	2.13	185.8	16.9	0.13	0.0113	-0.0021	0.0071	7	0.9	0.01
IC-6	XZ	45	0.99	1.96	2.17	195.3	18.3	0.11	0.0135	-0.0017	0.0101			
IC-9	XZ	45	0.99	1.96	2.18	199.1	18.6	0.12	0.0120	-0.0018	0.0084			
Average			0.99	1.96	2.16	193.4	17.9	0.12	0.0123	-0.0019	0.0085			
IB-3	YZ	45	0.99	2.01	2.20	178.2	18.5	0.11	0.0086	-0.0012	0.0062	12	0.1	0.01
IB-6	YZ	45	0.99	1.98	2.19	195.4	18.6	0.12	0.0107	-0.0016	0.0075			
Average			0.99	1.99	2.19	186.8	18.6	0.12	0.0096	-0.0014	0.0068			

XRD Results

Sample AE-4 (%)	XRD Mineral
88	Quartz
0	Albite
2	Plagioclase-Feldspar
3	Potassium-Feldspar
2	Mica-Illite-Smectite
0	Chlorite
4	Kaolinite
-	Calcite
-	Dolomite
-	Siderite
0	Pyrite
0	Anatase
0	Apatite
0	Halite
0	Anhydrite

- Trace amount

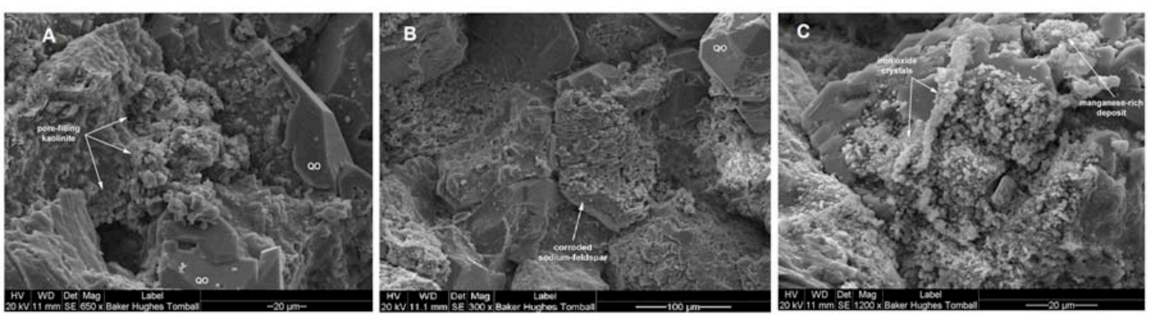

Figure 2: SEM showing (A) Pore-filling vermiculite kaolinite (B) Corroded sodium feldspar and (C) iron oxide crystals and manganese-rich deposit

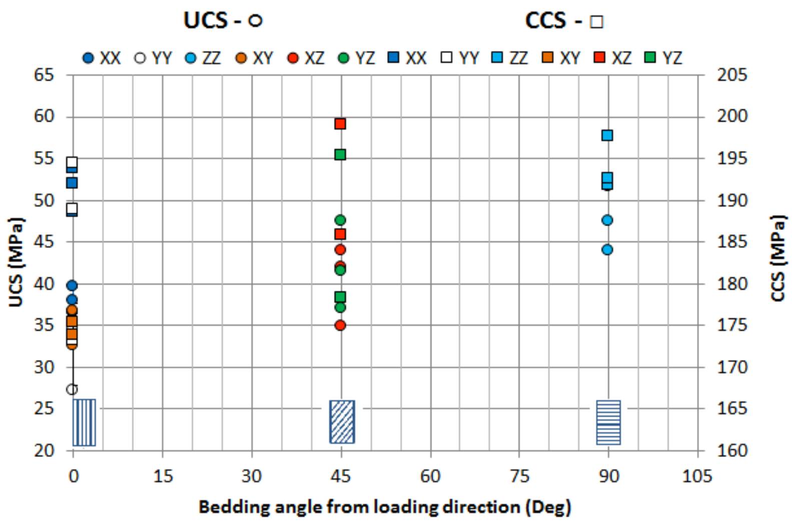

Figure 3: Effect of Bedding Plane on Unconfined and Confined Compressive Strength (UCS and CCS)

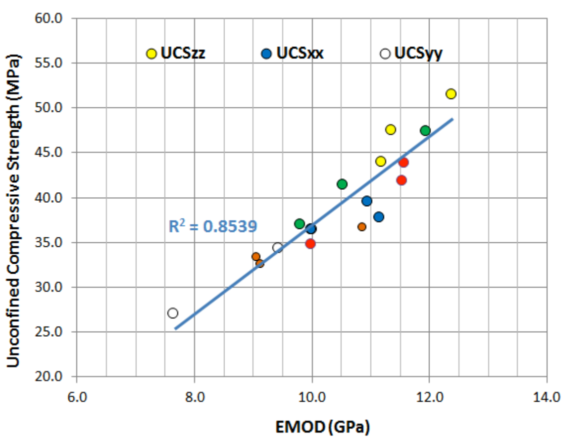

Figure 4: Young's Modulus at Uniaxial Testing Conditions (UCS) with respect to Bedding Plane From Loading Direction

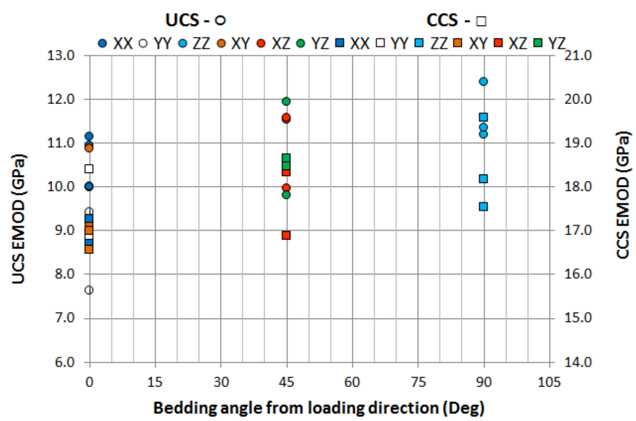

Figure 5: Effect of Bedding Plane on Young's Modulus during Uniaxial and Triaxial Testing Conditions (UCS and CCS)

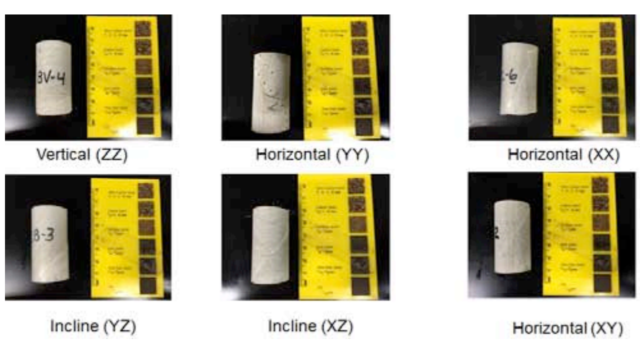

Figure 6: Shear Plane Failure Pattern on Post Triaxial Testing

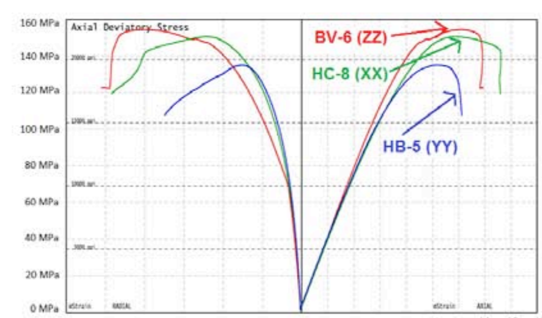

Figure 7: Stress-Strain Plots of Three Different Orientations to Bedding Plane